

Waves and instabilities in rotating free surface flows

J. Mougel ^a, D. Fabre^a, L. Lacaze^a, T. Bohr^b, L. Tophøj^b

a. Institut de Mécanique des Fluides de Toulouse,
Allée du Professeur Camille Soula, 31400 Toulouse, France

b. Physics Department, Technical University of Denmark, Lyngby, Denmark

Abstract :

The stability properties of the rotating free surface flow in a cylindrical container is studied using a global stability approach, considering succesively three models. For the case of solid body rotation (Newton's bucket), all eigenmodes are found to be stable, and are classified into three families : gravity waves, singular inertial modes, and Rossby waves. For the case of a potential flow, an instability is found. The mechanism is explained as a resonance between gravity waves and centrifugal waves, and is thought to be at the origin of the "rotating polygon instability" observed in experiments where the flow is driven by rotation of the bottom plate (see [9]). Finally, we give some preliminary results concerning a third model : the Rankine vortex.

1 Introduction

Rotating flows with a free surface are known to support rich dynamics. Spectacular examples are provided by a very simple experiment consisting of a cylindrical container partly filled with a liquid, in which the fluid motion is driven by a rapidly rotating bottom while the side wall is maintained fixed. For high enough rotation rates, a symmetry breaking is observed, leading to the formation of polygonal patterns rotating at a constant angular velocity on the free surface. This phenomenon, first observed in [10], has been revisited in [5] , [8], [1].

The objective of this paper is to give a brief summary of a research effort, conducted along the past two years, aiming at explaining those polygonal patterns as resulting from a linear instability of the axisymmetric flow predating them. For this purpose, we developed a global stability approach which allows to study the linear dynamics of various models of free surface swirling flows. After presenting the general method, we will review the results obtained with three successive models. First, in the case of a solid-body rotation, we observe only stable modes. However, the linear dynamics of this flows turn out to be rather interesting, as it involves singular modes displaying analogy with the inertial motion in rotating stars and spherical shells [7], and Rossby waves similar to those existing in a container with a non-flat bottom. Secondly, in the case of a potential rotation, we report the existence of an instability mechanism existing for all azimuthal wavenumbers $m \geq 2$. The mechanism is explained as a resonance between gravity waves and centrifugal waves, and was recently proposed to be at the origin of the aforementioned polygonal patterns [9]. Finally, we will show preliminary results obtained using an improved model combining an inner region in solid-body rotation and an outer region in potential rotation (Rankine model).

2 General equations

Using cylindrical coordinates (r, θ, z) , we consider a general azimuthal base flow of the form $\mathbf{U}_0 = U_\theta(r)\mathbf{e}_\theta$. The flow occupies a domain defined by $0 < r < R$ and $0 < z < h(r)$, where R is the radius of the cylindrical tank, and $h(r)$ is the altitude of the free surface. Neglecting the effect of surface tension, the shape of the free surface is related to the flow through the equation $\partial_r h = g_c/g$ where g is the gravity and $g_c = U_\theta^2/r$ is the centrifugal acceleration (this condition means that the free surface is perpendicular to the total acceleration $g\mathbf{e}_z + g_c\mathbf{e}_r$).

To investigate the stability of such flows we add small amplitude perturbations, under modal form, i.e.

$\epsilon[u, v, w, p, \eta]e^{i(m\theta - \omega t)}$, with m the azimuthal wave number and ω the complex frequency. The eigenmode structure has velocity and pressure $[u, v, w, p]$ components defined in the bulk (as function of r and z) while the component η corresponding to the vertical free surface displacement is defined on the boundary of the domain (function of r only). Restricting to the inviscid case¹, the linearized equations governing the dynamics of the perturbations are obtained from the Euler and continuity equations :

$$-i(\omega - m\frac{U_\theta}{r})u = -\partial_r p + 2\frac{U_\theta}{r}v, \quad (1a)$$

$$-i(\omega - m\frac{U_\theta}{r})v = -\frac{im}{r}p - \frac{1}{r}\frac{d(rU_\theta)}{dr}u, \quad (1b)$$

$$-i(\omega - m\frac{U_\theta}{r})w = -\partial_z p, \quad (1c)$$

$$\frac{\partial u}{\partial r} + \frac{u}{r} + \frac{im}{r}v + \frac{\partial w}{\partial z} = 0. \quad (1d)$$

On the bottom and side walls we apply non-penetration boundary conditions. At the free surface, we obtain linearized dynamic and kinematic boundary conditions of the form :

$$p + g\eta = 0; \quad -i(\omega - m\frac{U_\theta}{r})\eta = w - \partial_r u. \quad (2)$$

In the following we impose an analytical form for U_θ and perform a global stability analysis of this particular flow. In the finite element framework equations (1) and (2) can be written under the form of a generalized eigenvalue problem $AX = \omega BX$ with ω the eigenvalue, X the corresponding eigenmode and A and B complex matrices constructed with the finite element software FreeFem++. We note $\omega = \omega_r + i\omega_i$, where ω_r will refer to the oscillation frequency and ω_i to the growth rate. In particular $\omega_i > 0$ will denote instability.

3 Solid body rotation (Newton's Bucket)

The first case under investigation corresponds to a solid rotation of the whole liquid, corresponding to an azimuthal velocity profile of the form $U_\theta = r\Omega$. This flow can be parametrized by a Froude number $Fr = \Omega\sqrt{R/g}$ and a Reynolds number $Re = R^{3/2}\sqrt{g}/\nu$. It is a classical exercise to show that the free surface is parabolic. Assuming that the volume of liquid is conserved and equal to $\pi R^2 H$, where H is the liquid height at rest, one can further show that the bottom remains "wet" for $Fr < 2\sqrt{H/R}$ and gets "dry" above this threshold (see Figure 1(a)).

In the inviscid case one can reduce equations for the perturbation in the bulk (1) to a single equation for pressure which is known as Poincaré's equation :

$$\frac{\partial^2 p}{\partial r^2} + \frac{1}{r}\frac{\partial p}{\partial r} - \frac{m^2}{r^2}p + \left(\frac{(\omega - m\Omega)^2 - 4\Omega^2}{(\omega - m\Omega)^2}\right)\frac{\partial^2 p}{\partial z^2} = 0. \quad (3)$$

A well known feature of this equation is that the nature of the possible solutions change drastically depending on the relative frequency (with respect to the rotating frame) $\omega - m\Omega$ (see [3] for instance). Three cases have to be considered.

First, if $|\omega - m\Omega| > 2\Omega$, the equation is elliptic, and regular eigenmode solutions are expected to exist. Numerical results from the global stability analysis show that this is effectively the case, and Figure 1(b) shows that the solutions organize into two sets of branches. Figure 2(a) displays the typical structure of the corresponding eigenmodes : the structure is regular and the maximum pressure levels

¹The linearized equations in the general case, retaining viscosity and surface tension, are given in [6].

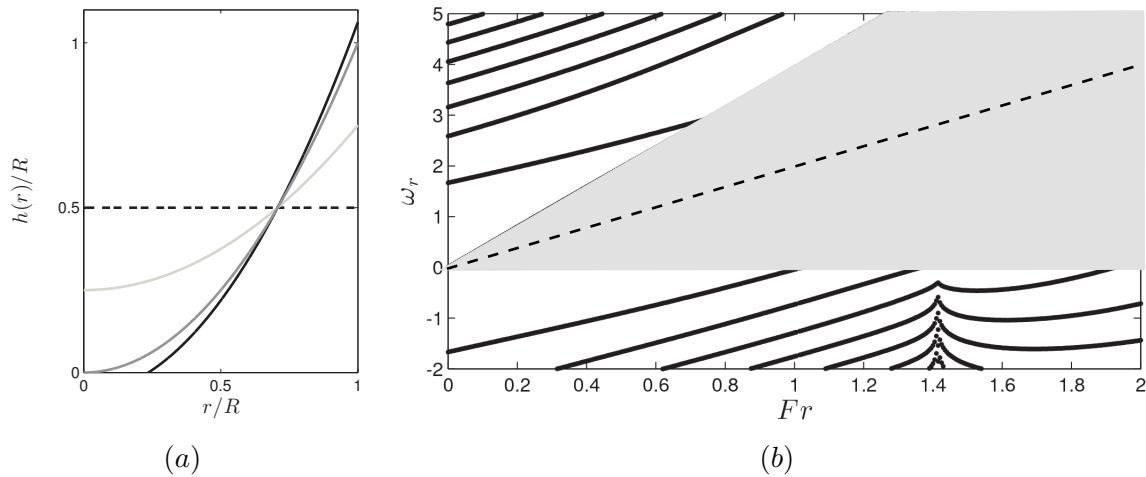


Figure 1: Solid body rotation (with $H/R = 0.5$) : (a) Shape of the free surface for $Fr = [1, \sqrt{2}, 1.5]$. (b) Oscillation rates of the normal modes as function of Fr , $m = 2$ (inviscid case). The black lines correspond to the regular *gravity waves* ; the grey area indicates the range of existence of the singular inertial modes, and the dashed line corresponds to $\omega = m\Omega$, in the vicinity of which the Rossby waves are found.

are located along the free surface. These modes are thus recognized as *gravity waves*, and in the limit of vanishing rotation ($Fr \approx 0$) their frequencies match with those of the pure sloshing modes in a cylindrical container with flat surface [4].

Secondly, if $|\omega - m\Omega|$ is smaller than 2Ω (but not too small compared to Ω), the Poincaré equation becomes hyperbolic. In such cases, regular eigenmode solutions are not expected to be met (except in the limit of small rotation where the surface becomes flat, and a separation of variables is possible). Instead, computations in the strictly inviscid case reveal the existence of a dense set of eigenfunctions corresponding to *singular inertial modes*. The range of existence of these singular eigenmodes is indicated by the shaded area in Figure 1(b). The singularity can be regularized by introducing a small amount of viscosity. Figure 2(b) displays the structure of a viscous mode obtained in this way (see [6] for details about the numerical implementation of the viscous case). Such modes are found to exhibit a striking ray-like structure, similar to the patterns observed in other configurations such as spherical shells [7], or rotating stars.

The third interesting case is met if the relative frequency $|\omega - m\Omega|$ is close to zero, i.e. when the perturbations are almost stationary with respect to the rotating frame. In this case, the Poincaré equation (3) becomes degenerate, and the Euler equations (1) reduce, at leading order, to the geostrophic equilibrium. In such a quasi-geostrophic context, variations of the height of liquid is known to allow for the possibility of a type of slow waves called *Rossby waves*. Such solutions are well known in the case where the variation of height is due to a non-flat bottom (see [3], pp. 85 for instance). In the present case, variation of height is also present because of the parabolic shape of the free surface, and the numerical results effectively demonstrates the existence of such Rossby waves. An example of such a wave is displayed in Figure 2(c). As can be seen, the structure of the mode (as displayed by the pressure component) is nearly independent of the vertical direction, which is a characteristic of flow motion in the quasi-geostrophic limit.

Note that as the rotation is increased, Figure 1(b) indicates that some of the branches of gravity waves enter the ‘hyperbolic’ interval. Complex interactions between the three kinds of modes are expected in this case. Another interesting feature is the discontinuity met along the branches of gravity waves at the wet/dry transition for $Fr = \sqrt{2}$. These features are the object of current investigations.

4 Potential rotation

Although the solid-body rotation model considered above seems the most natural model for the flow in a cylinder with a rotating bottom, experimental observations using PIV (see [1]) actually indicate

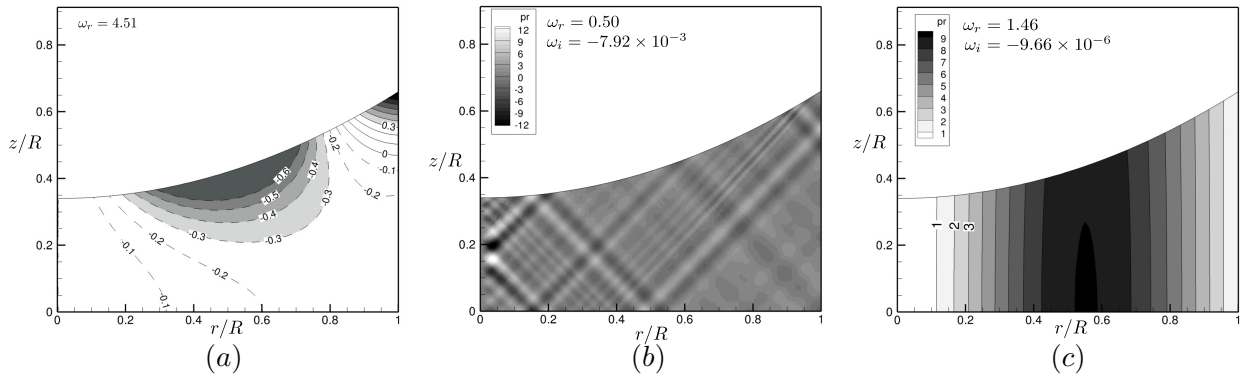


Figure 2: Solid-body rotation ($H/R = 0.5$): structure in the meridional plane of some eigenmodes (pressure component) obtained for $Fr = 0.8$, $H = 0.5$, $m = 2$. (a) Regular gravity wave (inviscid case). (b) Singular inertial mode with ray pattern. (c) Rossby wave. (plots (b) and (c) are viscous results with $Re = 10^{-7}$; here viscosity is introduced into the bulk equations only for sake of regularization).

that the potential rotation is a more appropriate model, especially in the cases with high rotation rate. We thus consider, as our second model, a potential model defined as $U_\theta(r) = \Gamma/(2\pi r)$ where Γ is the circulation. In this case the free surface is concave, with expression $h(r) = \Gamma^2/(8\pi^2 g) (1/\xi^2 - 1/r^2)$, where ξ is the radius of the central ‘dry’ region. The parameters Γ and ξ are related through the conservation of the volume of liquid, assuming again a total volume $\pi R^2 H$ where H is the liquid height at rest. Here we find more convenient to parametrize the results in terms of ξ/R and H/R .

In the global stability analysis, if we restrict to the inviscid case, we can take advantage of the potential nature of the base flow and assume the perturbation to be potential as well, leading to great simplifications in the analysis. Such a global analysis was carried out in [9], where it was shown that the potential flow is generically unstable to perturbations with wavenumbers $m > 1$.

In [9], we mostly focussed on the case ($H/R = 0.276$), which was documented in the experiments of [5]. In the present paper, we consider more particularly the case ($H/R = 0.94$), which corresponds to the experimental studies by [8]. In that experiment, only elliptical patterns ($m = 2$) have been observed. Figure 3(c) displays the amplification rates predicted by the global analysis in that case as function of ξ/R . It is found that instabilities with wavenumber $m = 2$ are by far the most amplified ones in this case, suggesting that the potential instability mechanism could also be at the origin of the observed patterns. Note that in the experiment, the elliptical patterns were found to alternate temporally with axisymmetric states, a phenomenon called ‘surface switching’. This phenomenon is certainly non linear and thus cannot be predicted by our approach.

Figure 3(b) displays the real part of the frequency (for the same conditions as in Figure 3(c)), restricting to the case $m = 2$. This figure illustrates the fact that instabilities arise in ranges of ξ corresponding to the crossing between two families of branches. In [9], we argued that these two families of branches actually correspond to two different kinds of surface waves : the branches going upwards are *gravity waves*, since the restoring force responsible for them is the gravity acting on the external part of the free surface where it is nearly horizontal, while the branches going downwards are *centrifugal waves* since in their case the restoring force is the centrifugal effect acting on the inner part of the free surface where it is nearly vertical.

For particular values of ξ we see that two waves of each type can resonate. It has been shown that this resonant behaviour either lead to an instability creating two complex conjugate modes during the merging or to a stable no-merging process where both waves exchange identities. The selection of the crossing process is related to the energy of both waves as defined in [2] and an instability can be found only if one wave has negative energy and the other positive energy (here a wave having negative energy means that the system wave+base flow has less energy than the base flow). In [9] it is found using Cairns terminology (see [2]) and a simple 2D model that the energy of the gravity and centrifugal

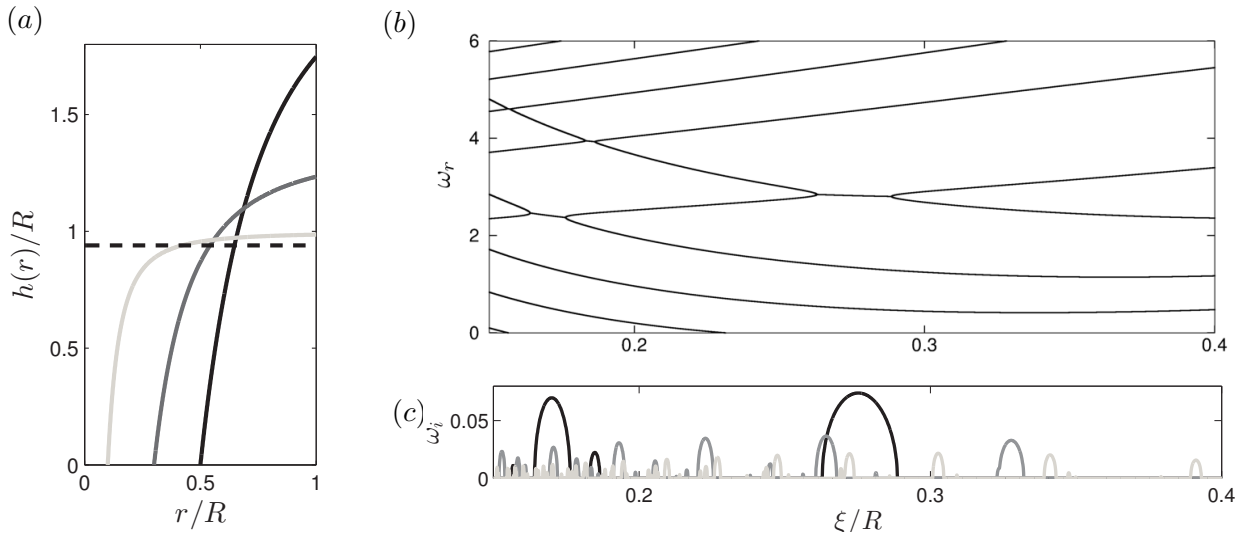


Figure 3: Potential rotation (with $H/R = 0.94$): (a) Shape of the free surface for $\xi/R = [0.1, 0.3, 0.5]$. (b) Oscillation rates ω_r for $m = 2$. (c) Growth rate ω_i for $m = 2$ (black), $m = 3$ (dark grey) and $m = 4$ (light grey).

waves respectively read $E_g \sim (\omega - mU_\theta(R)/R)$ and $E_c \sim (\omega - mU_\theta(\xi)/\xi)$. These expressions mean that the centrifugal waves should be slower than the base flow and the gravity waves faster for the instability to occur (i.e. existence of a critical radius $r_c \in [\xi, R]$ where the global mode and the base flow have the same angular velocity).

From Figure 3(c), it can be noted that instability ‘bubbles’ get much narrower when m increases and in fact the maximum growth rate decreases rapidly. This fact is confirmed by an ongoing asymptotic study, conducted in the shallow water limit, which indicates a trend with the form $\omega_{i,max} = e^{-Cm} \sqrt{m}$ with $C > 0$. Thus the fact that no polygons with more than 6 corners are observed experimentally ([10], [5]) could simply mean that the theoretical instability obtained in the potential case is too weak to be observed in the real setup for these values of m .

5 Rankine Vortex

A drawback of the potential model considered in the previous section is that the free surface necessarily touches the bottom at some location $r = \xi$ (see Figure 3(a)), so it certainly cannot account for the ‘wet’ states observed experimentally at low or moderate values of the rotation rate. Indeed, in such cases, the experimental results of [1] indicate that in the central region of the container, the motion is actually close to a solid-body rotation. This leads one to introduce an improved model combining an inner core in solid body rotation and an outer potential zone (Rankine vortex). The velocity of this base flow then reads

$$U_\theta = \Omega r \quad \text{for } 0 < r \leq a, \quad U_\theta = \frac{\Gamma}{2\pi r} \quad \text{for } a < r < R, \quad (4)$$

with a the radius of the vortex core, and $\Gamma = 2\pi\Omega a^2$ (assuming continuity at $r = a$). In the following our parameter will be $Fr = \Omega\sqrt{R/g}$, and we will fix $a/R = 0.5$ and $H/R = 0.5$. Figure 4(a) displays the shape of the corresponding free surface. The boundary of the vortical core at $r = a$ is associated with a change of curvature of the free surface, from concave to convex. With the chosen parameters, the wet/dry transition occurs at $Fr \approx 1.77$.

The global stability analysis of this flow is currently ongoing, and preliminary results for $m = 2$ are displayed in figure 4(b – c). Figure 4(b) depicts the oscillation frequencies of the modes as function of Fr . The results show some similarity with those obtained in the case of solid-body rotation (not surprisingly, since the Poincaré equation also holds in the inner zone in solid body rotation). As

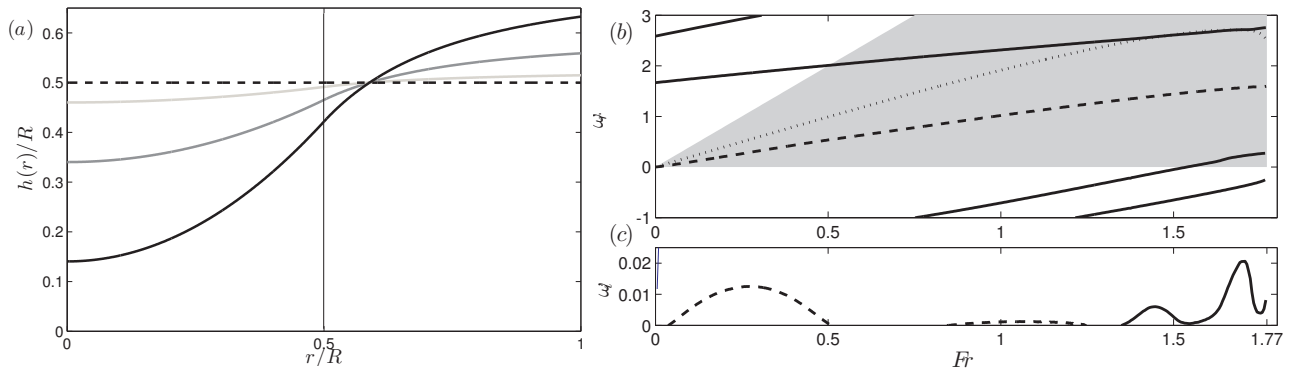


Figure 4: Rankine model (with $H/R = a/R = 0.5$): (a) Shape of the free surface for $Fr = [0.5, 1, 1.5]$ (the vertical line separates the vortex core from the outer potential zone). (b) Oscillation frequencies ω_r of some of the wave solutions encountered in the global stability analysis for $Re = 10^{-4}$ (full lines : gravity waves ; dashed line : regular Kelvin wave ; dotted line : Rossby wave ; grey area : range of existence of singular inertial waves). (c) Growth rates of the two encountered unstable modes.

previously, we observe the existence of regular gravity waves (plain lines), a dense set of singular modes (grey area), and some Rossby-like waves in the range $\omega \approx m\Omega$ (dashed line). In addition, we also observed a new branch with a different nature, with a frequency following approximatively the trend $\omega \approx (m - 1)\Omega$. This trend, as well as the structure of the corresponding mode, leads us to identify this branch with the well-known two-dimensional Kelvin wave solution.

Preliminary results show that (at least) two branches of eigenmodes lead to instability, and the corresponding growth rates are displayed in Figure 4(c). One of them is observed for high rotations (namely $Fr > 1.35$), and is likely due to a resonance between a gravity wave and a Rossby-like wave. The second is met for smaller rotations and corresponds to the ‘Kelvin Wave’ ; the mechanism leading to instability of this branch is still unknown.

More complete results will be presented in due course, as for the structure of these new kinds of unstable modes, the underlying physics, and their relevance with the experimentally observed polygonal patterns.

References

- [1] Bergmann, R., Tophøj, L., Homan, T. A. M., Hersen, P., Andersen, A. and Bohr, T. 2011 Polygon formation and surface flow on a rotating fluid surface. *Journal of Fluid Mechanics* **679** 415-431
- [2] Cairns, R. A. 1979 The role of negative energy waves in some instabilities of parallel flows. *Journal of Fluid Mechanics* **92** 1-14
- [3] Greenspan, H. P. 1969 The theory of rotating flows. *Cambridge Univ. Press*
- [4] Ibrahim, R.A. 2005 Liquid Sloshing Dynamics. *Theory and Applications*. *Cambridge Univ. Press*
- [5] Jansson, T.R.N., Haspang, M.P., Jensen, K.H., Bohr, T 2006 Polygons on a Rotating Fluid Surface. *Phys. Rev. Lett.* **96** 174502
- [6] Mougel, J. 2011 Etude de stabilité linéaire du seau de Newton. *Mémoire de stage de Master, ISAE*.
- [7] Rieutord, M. and Valdettaro, L. 1997 Inertial waves in a rotating spherical shell. *Journal of Fluid Mechanics* **341** 77-99
- [8] Suzuki, T., Iima, M. and Hayase, Y. 2006 Surface switching of rotating fluid in a cylinder. *Physics of Fluids*, **18** 101701
- [9] Tophøj, L., Mougel, J., Bohr, T., Fabre, D. 2013 The Rotating Polygon Instability of a Swirling Free Surface Flow. *Phys. Rev. Lett.* (submitted)
- [10] Vatistas, G. H. 1990 A note on liquid vortex sloshing and Kelvin’s equilibria. *Journal of Fluid Mechanics* 241-248